

Thermal Rectification and Negative Differential Thermal Resistance in a driven two segment classical Heisenberg chain

Debarshee Bagchi

Theoretical Condensed Matter Physics Division, Saha Institute of Nuclear Physics,
1/AF Bidhannagar, Kolkata 700064, India

E-mail: debarshee.bagchi@saha.ac.in

Abstract. We investigate thermal transport in a two segment classical Heisenberg spin chain with nearest neighbor interaction and in presence of external magnetic field using computer simulation. The system is thermally driven by heat baths attached at the two ends and transport properties are studied using an energy conserving dynamics. We demonstrate that by properly tuning the parameters thermal rectification can be achieved - the system behaves as a good conductor of heat along one direction but becomes a bad conductor when the thermal gradient is reversed and crucially depends on nonlinearity and spatial asymmetry. Moreover, suitable tuning of the system parameters gives rise to the counterintuitive and technologically important feature known as the negative differential thermal resistance (NDTR). We find that the crucial factor responsible for the emergence of NDTR is a suitable mechanism to impede the current in the bulk of the system.

PACS numbers: 75.10.Hk, 44.10.+i, 66.70.Hk, 05.60.Cd

1. Introduction

Thermal management in low dimensional mesoscopic systems is an active topic of research at present. The quest to manipulate and control heat current, just as one can do with electrical current in electronic devices, has given birth to an altogether new branch of study namely the *phononics* [1, 2]. Needless to say, these studies are important not only in understanding the principles of low dimensional thermal transport, for example, necessary and sufficient condition for Fourier law [3, 4, 5], but also have immense technological application in today's world. Phononics deals with the manipulation of thermally excited phonons in the system and is now quite a mature field of research. Designs for many useful thermal devices have been proposed in recent times such as the thermal rectifier [6, 7], transistor [8], logic gates [9], memory elements [10], current limiter and constant current source [11]. In fact, very recently a thermal rectifier [12] and a thermal wave guide [13], both using carbon and boron nitride nanotubes, have been successfully fabricated in the laboratory. Apart from phonons, spin waves (magnons) in magnetic systems are also known to be an efficient mode of energy transport for quite some time now [14]. Although considerable progress has been achieved in understanding magnon assisted thermal transport [15], a lot of effort still needs to be devoted before this can be utilized in real thermal devices.

The Heisenberg model [16, 17] is a paradigmatic model for magnetic insulators. Thermal transport properties of the one dimensional classical Heisenberg model have been studied in recent times and it is now known that in the thermodynamic limit heat transport in this model obeys Fourier law (diffusive transport of energy) for all temperature and magnetic field [18, 19]. This diffusive energy transport is attributed to the nonlinear spin wave interactions in this model which cause spin waves to scatter [18]. However, for finite systems there can be a crossover from ballistic to diffusive behavior which crucially depends on the temperature [19] and also on other system parameters such as an external magnetic field. This is due to the fact that at very low temperature or very high magnetic field the entire system becomes correlated and heat energy can pass from the hotter to the colder end without being scattered.

In this paper we study the thermal transport in a two segment classical Heisenberg spin chain. The two segments are connected to each other by a link and external magnetic fields act on the spins in the chain. Heat baths are attached to the two ends of the system and an energy current flows through the system in response to the imposed thermal gradient. It is found that the thermal current can be rectified by suitably tuning the system parameters. Thus heat current can preferentially flow through the system along one direction while it is inhibited in the opposite direction i.e., when the thermal gradient is reversed.

Over the last decade, thermal rectification has been intensively investigated in a large number of theoretical as well as experimental works and in a variety of systems; for a recent review see [20]. Thermal rectification has been observed in many classical nonlinear asymmetric lattices in one dimension with different forms of interaction

potentials e.g., Morse [6, 21], FK [7, 22], FK-FPU [23], graded mass harmonic systems [24, 25] to name a few. Studies of thermal rectification in two [26] and three [27] dimensions have also been done recently.

Another counterintuitive feature that emerges in some of these systems is the negative differential thermal resistance (NDTR) [7]. In the NDTR regime thermal current through a driven system is found to decrease as the imposed thermal gradient is increased. Although a lot of work [28, 29, 30, 31, 32] has been done to figure out the criteria responsible for the origin of NDTR, a comprehensive understanding is still lacking. This is however highly desirable now, since NDTR is a promising feature and is believed to be crucial in the functioning of thermal devices, such as thermal transistors [8] and thermal logic gates [9].

In this paper we focus particularly on these two features - thermal rectification and negative differential thermal resistance. Rectification and NDTR have been observed using computer simulation for the classical two dimensional Ising spin system [33]. Although rectification was attributed to the difference in the temperature dependence of thermal conductivity of the two segments, the origin of the intriguing NDTR effect was not discussed. Also there are certain differences between the Ising system and our chosen spin model. Firstly, Ising model is a discrete spin model and, although simple, it is not very realistic. A more realistic spin model is the Heisenberg model with continuous spin degree of freedom. Secondly, the 2d Ising model has a phase transition at a finite temperature whereas, the 1d Heisenberg model does not have a phase transition at any finite temperature. However thermal transport is found to be diffusive (obeys Fourier law) for both the models. Since an exact analytical treatment is generally not possible for most of the models mentioned above, an effective alternative is to investigate different generic models using numerical simulation. In the present work, we undertake such a numerical study of the above-mentioned features in a driven classical Heisenberg spin system.

The organization of the paper is as follows. We define the two segment classical Heisenberg spin chain in detail in Sec. 2. The simulation of the model has been performed using the discrete time odd even (DTOE) dynamics. The numerical implementation of this dynamics is briefly discussed in Sec. 3. Thereafter in Sec. 4, we present our numerical results and demonstrate the existence of thermal rectification and negative differential thermal resistance in this system. We study dependencies of system parameters on these features and also investigate the underlying physical mechanism for the emergence of the NDTR regime. Finally, we conclude by summarizing our main results and with a discussion in Sec. 5.

2. Model

A schematic diagram of the model studied here is shown in Fig. 1. Consider two one-dimensional segments of spins connected to each other by a link. The spins \vec{S}_i^L (\vec{S}_i^R) are conventional classical Heisenberg spins belonging to the left (right) segment of the

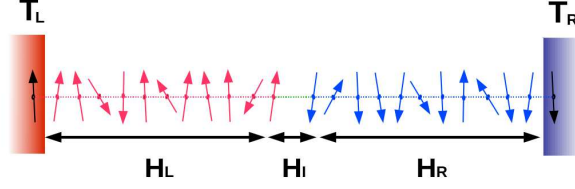


Figure 1. (Color online) Schematic diagram of the two segment classical Heisenberg model.

chain and i is the site index which runs from $1 \leq i \leq N_L(N_R)$. Each spin on the left (right) segment interacts with an external magnetic field \vec{h}_i^L (\vec{h}_i^R). The Hamiltonian of the system is given as,

$$\mathcal{H} = \mathcal{H}_L + \mathcal{H}_I + \mathcal{H}_R \quad (1)$$

and the interaction of the spins in the left and the right segments are

$$\begin{aligned} \mathcal{H}_L &= -K_L \sum_{i=1}^{N_L-1} \vec{S}_i^L \cdot \vec{S}_{i+1}^L - \sum_{i=1}^{N_L} \vec{h}_i^L \cdot \vec{S}_i^L \\ \mathcal{H}_R &= -K_R \sum_{i=1}^{N_R-1} \vec{S}_i^R \cdot \vec{S}_{i+1}^R - \sum_{i=1}^{N_R} \vec{h}_i^R \cdot \vec{S}_i^R, \end{aligned} \quad (2)$$

where the K 's are the interaction strengths which is ferromagnetic for coupling $K > 0$ and anti-ferromagnetic for $K < 0$. The interaction of the last spin of the left segment $i = N_L$ and the first spin of the right segment $i = 1$ is chosen to be of the ferromagnetic Ising-Heisenberg form [34]

$$\mathcal{H}_I = -K_I \left[\lambda (S_i^x S_j^x + S_i^y S_j^y) + S_i^z S_j^z \right], \quad (3)$$

where $\vec{S}_i = \vec{S}_{N_L}^L$ and $\vec{S}_j = \vec{S}_1^R$ which defines the link connecting the two segments. For $\lambda = 1$, we refer to the interaction at the interface as the (isotropic) ‘‘Heisenberg’’ type, whereas, for $\lambda = 0$, the ‘‘Ising’’ type. For intermediate values of λ we have (anisotropic) ‘‘XXZ’’ type interaction at the interface. Note that the spins are free to fluctuate in all the three directions for all λ .

The evolution equation for the spin vectors in the two segments can be written as,

$$\frac{d}{dt} \vec{S}_i = \vec{S}_i \times \vec{B}_i, \quad (4)$$

where $\vec{B}_i = (K_i^- \vec{S}_{i-1} + K_i^+ \vec{S}_{i+1}) + \vec{h}_i$ is the local molecular field experienced by the spin \vec{S}_i ; K_i^- and K_i^+ are the interactions of \vec{S}_i with \vec{S}_{i-1} and \vec{S}_{i+1} respectively and will be K_L , K_R or K_I depending on the segment in which the spins \vec{S}_{i-1} , \vec{S}_i and \vec{S}_{i+1} belong to; \vec{h}_i is the magnetic field acting on the i -th spin. For the two spins at the interface the equation of motion can be written down analogously.

This two segment system is thermally driven by two heat baths attached to the two ends. This is numerically implemented by introducing two additional spins at sites

$i = 0$ on the left segment and $i = N_R + 1$ on the right segment. The bonds between the pairs of spins $(\vec{S}_0^L, \vec{S}_1^L)$ and $(\vec{S}_{N_R}^R, \vec{S}_{N_R+1}^R)$ at two ends of the system behave as stochastic thermal baths [19]. The interaction strength of the bath spins with the system is taken to be K_b , and therefore energy of both the baths is bounded in the range $(-K_b, K_b)$ and has a Boltzmann distribution. Thus the left and right baths are in equilibrium at their respective temperatures, T_L and T_R with average energies $E_L = -K_b \mathcal{L}(K_b/T_L)$ and $E_R = -K_b \mathcal{L}(K_b/T_R)$, $\mathcal{L}(x)$ being the standard Langévin function. Thus one can set the two baths at a fixed average energies (or fixed temperatures) and an energy current flows through the system if $T_L \neq T_R$. In the steady state a uniform current (independent of the site index i) transports thermal energy from the hotter to the colder end of this composite system.

3. Numerical Scheme

We investigate transport properties of this composite two segment Heisenberg model by numerically computing the steady state quantities, such as, currents, energy profiles etc. using the energy conserving DTOE dynamics [19, 35]. The DTOE dynamics updates spins belonging to the odd and even sub-lattices alternately using a spin precessional dynamics

$$\vec{S}_{i,t+1} = \left[\vec{S} \cos \phi + (\vec{S} \times \hat{B}) \sin \phi + (\vec{S} \cdot \hat{B}) \hat{B} (1 - \cos \phi) \right]_{i,t} \quad (5)$$

where $\hat{B}_i = \vec{B}_i/|\vec{B}_i|$, $\phi_i = |\vec{B}_i|\Delta t$ and Δt is the integration time step. The above formula is sometimes referred to as the *rotation formula* and holds for any finite rotation [36]. Note that Eq. 5 reduces to the equation of motion Eq. 4 in the limit $\Delta t \rightarrow 0$. The bath spins are refreshed by drawing the bond energies between the spins $(\vec{S}_0^L, \vec{S}_1^L)$ and $(\vec{S}_{N_R}^R, \vec{S}_{N_R+1}^R)$ from their respective Boltzmann distribution consistent with the temperature of the left and right bath temperatures. The left bath (at $i = 0$) is updated along with the even spins and the right bath is updated along with the even or odd spins depending on whether $i = N_R + 1$ is even or odd.

The DTOE dynamics alternately updates only half of the spins (odd or even) but all the bond energies are updated simultaneously. So the energy of the i -th bond ε_i^o measured immediately after the update of odd spins is not equal to its bond energy ε_i^e measured after the subsequent update of even spins, where we define the energy density $\varepsilon_i = -\vec{S}_i \cdot [K_i^+ \vec{S}_{i+1} + \vec{h}_i]$. The difference $\varepsilon_i^e - \varepsilon_i^o$ is the measure of the heat energy passing through the i -th bond in time Δt . Therefore the current J (rate of flow of energy) in the steady state is given by

$$J = \langle \varepsilon_i^e - \varepsilon_i^o \rangle / \Delta t. \quad (6)$$

Note that Eq. (6) can be shown to be consistent with the definition of current obtained using the continuity equation [19]. Numerically however, the current J can be computed as

$$J = -K_i^+ \langle (\vec{S}_i \cdot \vec{S}_{i+1})^e - (\vec{S}_i \cdot \vec{S}_{i+1})^o \rangle / \Delta t, \quad (7)$$

since the magnetic field term cancels out in the above expression. The energy profile E_i for sites in the two segments is computed as

$$E_i = - \left\langle \frac{1}{2} \vec{S}_i \cdot (K_i^- \vec{S}_{i-1} + K_i^+ \vec{S}_{i+1}) + \vec{h}_i \cdot \vec{S}_i \right\rangle, \quad (8)$$

For the left and the right boundaries (bath sites) energy is calculated as,

$$E_L = -K_b \langle \vec{S}_0^L \cdot \vec{S}_1^L \rangle \quad E_R = -K_b \langle \vec{S}_{N_R}^R \cdot \vec{S}_{N_R+1}^R \rangle. \quad (9)$$

In the following we present our numerical results obtained using the DTOE dynamics for the thermally driven two segment classical Heisenberg model.

4. Numerical Results

We study the two segment system with boundary temperatures $T_L = T_0(1 + \Delta)$ and $T_R = T_0(1 - \Delta)$; the average temperature of the system can be taken as $\frac{1}{2}(T_L + T_R) = T_0$. We set the segment sizes $N_L = N_R = N$, and the parameters are set as $K_b = K_L = 1$, $K_R = K$, $\vec{h}_i^L = (0, 0, 1)$ $\vec{h}_i^R = (0, 0, h)$. Thus the parameters we can manipulate reduce to Δ, K, h and the interface parameters (K_I, λ) , all of which are kept restricted in the range $(0, 1)$ unless mentioned otherwise. The time step Δt is chosen relatively larger since a larger Δt ensures faster equilibration of the system and because energy conservation is maintained for any finite Δt [19]. Also it can be shown that the final stationary state is the same for all choices of Δt [19]. In the following we set $\Delta t = 2.0$ for all our simulations. Starting from a random initial configuration we evolve the spins using the DTOE dynamics. Once a nonequilibrium stationary state is reached, we compute various quantities, such as, the thermal current and the energy profiles for different values of the above mentioned parameters, temperature and system size.

4.1. Thermal rectification

First, we consider the system with $\lambda = 1$ (“Heisenberg” type interaction at the interface) and study the thermal current through the system for different values of the parameter $-1 < \Delta < 1$. A positive Δ implies that $T_L > T_R$, whereas, the same Δ with a negative sign implies that the heat baths have been swapped between the two ends. We refer to $\Delta > 0$ as the forward bias and $\Delta < 0$ as the backward bias. Thus the entire system is now a Heisenberg spin chain with spatial asymmetry due to dissimilar spin-spin coupling strengths and magnetic fields in the two segments. The variation of the thermal current with the bias Δ for different values of average temperature T_0 is shown in Fig. 2a. We find that the thermal current is considerably larger for $\Delta > 0$ whereas, for the same value of Δ but with the baths interchanged, the current through the system is smaller. Thus, this nonlinear asymmetric two segment system behaves as a thermal rectifier i.e., it acts as a good conductor of heat in one direction and as a bad conductor in the reverse direction. Evidently this rectification effect is more pronounced at lower temperatures as can be seen in Fig. 2a.

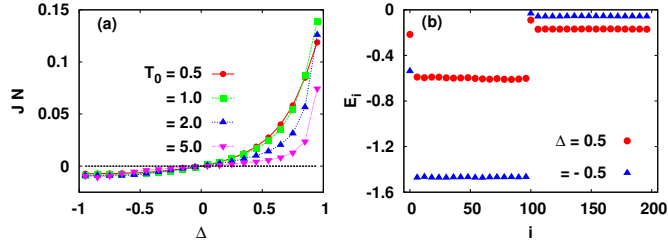


Figure 2. (Color online) (a) Variation of the thermal current J with Δ for different average temperatures $T_0 = 0.5, 1.0, 2.0$ and 5.0 . (b) Energy profile of the system for $\Delta = 0.5$ and -0.5 ; average temperature $T_0 = 1.0$. The parameters used for both the figures are $\lambda = 1$, $K = 0.5$, $K_I = 0.05$, $h = 0.1$ and segment size $N = 100$.

The steady state energy profiles of this two segment system is displayed in Fig. 2b. for $\Delta = 0.5$ and -0.5 . It can be seen that the energy profile is almost flat implying that the system is near the ballistic regime, and there is an energy jump at the interface. This energy discontinuity is due to the interface thermal resistance, often referred to as the *Kapitza resistance* [37]. The current that flows in the system depends essentially on two factors namely the imposed bias and the interface resistance. The current increases as the bias is increased but decreases if the interface resistance is high which diminishes the current carrying capacity of the lattice i.e., its conductivity drops. It can be seen from Fig. 2b that the interface resistance is comparatively larger for $\Delta = -0.5$ than for $\Delta = 0.5$. This disparity in the interface resistance along the forward and the backward direction for the same bias magnitude $|\Delta|$ results in the rectification of the thermal current. Thus in such nonlinear systems, the interface resistance is a function of the imposed driving field and has unequal values in the forward and the backward direction due to the spatial asymmetry of the lattice.

To quantify the amount of rectification, we compute the rectification efficiency defined as $\eta = |J_+/J_-|$ where both the forward and the backward currents, J_+ and J_- , are computed for the same $|\Delta|$. The variation of the rectification efficiency for $|\Delta| = 0.25, 0.5$ and 0.75 is shown in Fig. 3 for different values of average temperature T_0 , magnetic field h , interface coupling K_I and segment size N . The rectification is found to decrease as the temperature, interface coupling strength and the system size increases. With magnetic field, the efficiency has a non-monotonic dependence in the range $0 < h < 1$. It first increases and attains a maximum value corresponding to the field value h^* (say) and decreases thereafter decreases in the range $h^* < h < 1$. From the temperature and the system size data it is clear that rectification is more when the system is closer to the ballistic regime (lower temperature and smaller system size). As the magnetic field increases from zero, the system moves closer to the ballistic regime and thus efficiency η increases. However, as h approaches unity, there is a drop in the efficiency since the asymmetry of the system is gradually lost. Thus the non-monotonicity of the $\eta \sim h$ curve is related to this interplay between ballistic-diffusive transport processes and asymmetry of the lattice. The efficiency attains a maximum

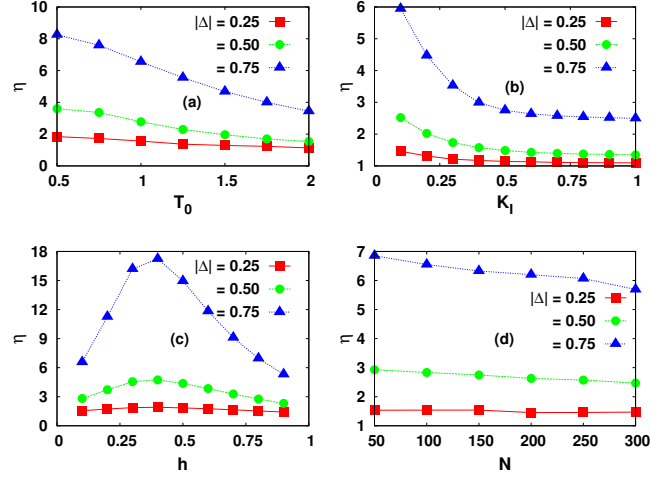


Figure 3. (Color online) The variation of rectification efficiency η with (a) average temperature T_0 (b) interface coupling K_I (c) magnetic field strength h and (d) segment size N is shown for $|\Delta| = 0.25, 0.5$, and 0.75 . The values of the parameters are chosen as $T_0 = 1.0$, $K_I = 0.05$, $h = 0.1$, $K = 0.5$ and $N = 100$. In each plot only one of the above parameters is varied keeping all other values the same.

value when both these factors have an optimum value. If h is increased beyond unity the rectification will again start to increase due to spatial asymmetry. Since here rectification can be controlled externally by tuning the magnetic fields, one can achieve quite large rectification efficiency in this system.

Microscopically, if one looks at the two spins at the interface, namely \vec{S}_N^L and \vec{S}_1^R , it is observed that the spins have unequal rotational *stiffness* for the forward and backward bias. By stiffness we mean the extent of rotation that is allowed for a particular spin about the \hat{z} -axis i.e., the angle θ which is in the range $0 \leq \theta \leq \pi$. If a spin \vec{S}_i can rotate completely freely then $S_i^z = \cos \theta$ should be a uniform distribution in the range $-1 \leq \cos \theta \leq 1$ with zero mean. However, if the spin is constrained to rotate within a restricted angle then the mean $\langle \cos \theta \rangle$ is nonzero. For such a case, the larger the magnitude of $\langle \cos \theta \rangle$ the more is the stiffness of the spin and less will be the current that passes through the i -th site. In Fig. 4, we show the steady state distribution $P(\cos \theta)$ for the two spins at the interface for $|\Delta| = 0.5$, both in the forward and backward bias.

We find that the distribution for the spin on the right segment \vec{S}_1^R does not change much in the forward and the backward bias. However the distribution for the left spin \vec{S}_N^L changes appreciably and the ratio $\langle \cos \theta \rangle_- / \langle \cos \theta \rangle_+ \approx 2.5$. Although this is rather crude, it gives a fairly good estimate of the amount of rectification achieved from the system for the given set of parameter values as presented in Fig. 2a ($J_+/J_- \approx 2.8$ for $|\Delta| = 0.5$ at $T_0 = 1.0$). Note that, this unequal spin stiffness is also the reason for the unequal energy discontinuity at the interface for the forward and backward bias, as shown in Fig. 2b. From the numerical data we estimate the ratio of the interface energy jumps $\Delta E_- / \Delta E_+ \approx 3.0$. The left segment's stiffness dominates over that of the right segment because of the higher values of interaction strength and

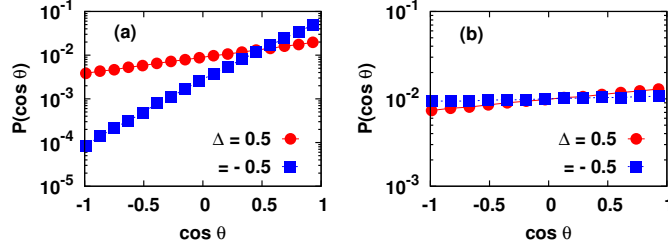


Figure 4. (Color online) Semi-log plot of the distribution of $\cos \theta$ (or the \hat{z} component of the spin) of spins (a) \vec{S}_N^L and (b) \vec{S}_1^R , for forward and backward bias. Here $\lambda = 1$, $|\Delta| = 0.5$ and $T_0 = 1.0$; other parameters are the same as in Fig. 2.

magnetic field in the former. This disparity in spin stiffness at the interface inhibits the current in the backward bias condition and gives rise to thermal rectification. This also explains the parameter dependencies of the rectification ratio η which decreases as temperature, interface coupling and system size increases, and the magnetic field decreases (for $0 < h < h^*$) since all these factors result in the decrease of spin stiffness at the interface.

4.2. Thermal rectification and NDTR

Next, we set the parameter $\lambda = 0$ and therefore now there is an “Ising” type interaction at the interface of the two segments. We study the thermal current J for different values of the parameter Δ keeping all other parameters the same as in the previous case. The result obtained from simulation is displayed in Fig. 5a. The rectification feature is again seen in this case - the forward current (for $\Delta > 0$) is appreciably larger in magnitude than the backward current (for $\Delta < 0$). The energy profiles for different values of Δ is shown in Fig. 5b. The rectification effect here can be again explained as in the previous case.

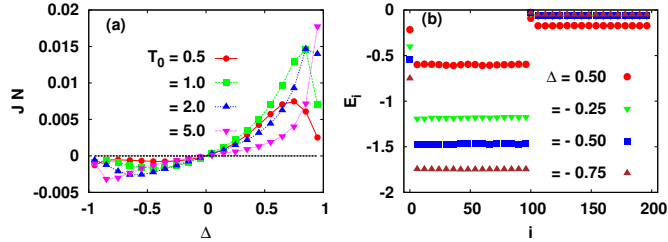


Figure 5. (Color online) (a) Variation of the thermal current J with Δ for different average temperatures $T_0 = 0.5, 1.0, 2.0$ and 5.0 . (b) Energy profile of the system for $\Delta = 0.5$ and $-0.25, -0.5, -0.75$; average temperature $T_0 = 1.0$. Here $\lambda = 0$ and all other parameters are the same as in Fig. 2.

In addition, careful observation reveals that for certain regions of the $J \sim \Delta$ curves in Fig. 5a, the current actually decreases as $|\Delta|$ is increased. Thus unlike the case of

$\lambda = 1$, where the magnitude of the current J appears to be a strictly non-decreasing function of the parameter Δ , for $\lambda = 0$ it is a non-monotonic function. This feature can be seen in certain ranges for all the four $J \sim \Delta$ curves shown in Fig. 5a. This is known as the *negative differential thermal resistance* (NDTR). In the following, we discuss in detail the NDTR feature seen here and try to understand how different factors influence the emergence of the NDTR region.

We focus on the $\Delta < 0$ region of the $J \sim \Delta$ curve and first study the parameter dependencies of the NDTR feature. Since it is difficult to compare NDTR regimes for different parameters and system sizes directly (because the current has different typical values), we define a quantity $\gamma \equiv (J_{m+1} - J_m)/J_m$ which is essentially the change in the thermal current scaled by the typical value of the current, for two consecutive discrete values of Δ belonging to $\{\Delta_m\}$ where $1 \leq m \leq M$, M being the total number of Δ values for which the current has been numerically computed. Note that if $|\Delta_{m+1}| > |\Delta_m|$ then γ is positive for positive differential thermal resistance (PDTR) and negative in the NDTR regime. Thus γ indicates the onset and also the width of the NDTR regime.

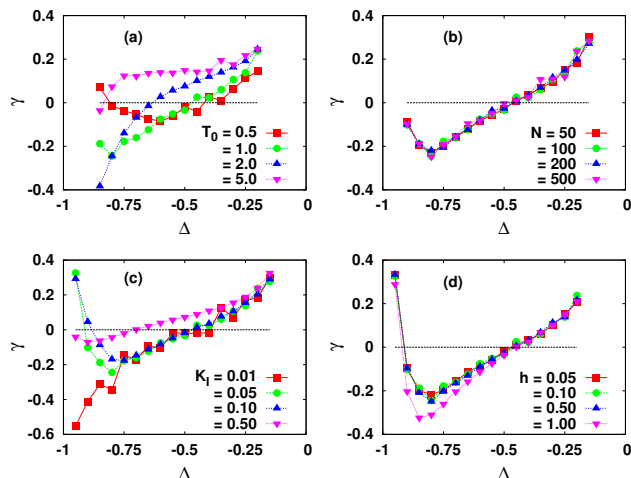


Figure 6. (Color online) Variation of γ with Δ for different (a) average temperature T_0 (b) segment size N (c) interface coupling K_I and (d) magnetic field strength h . The values of the parameters are set as $K = 0.5$, $T_0 = 1.0$, $K_I = 0.05$, $h = 0.1$, and $N = 100$, and only one of the parameters is varied in each of the above plots.

In Fig. 6 we show the quantity γ with Δ for different parameters T_0 , h , K_I and size N . We find that the NDTR regime sets in for smaller Δ values at lower average temperature T_0 and the NDTR region vanishes as T_0 is increased. It is also found that NDTR is more pronounced for smaller values of the interface coupling K_I . With system size the NDTR regime remains unaffected which is strikingly different from the result obtained for generic nonlinear models where the NDTR regime vanishes for larger sizes [28]. Thus for a wide range of segment sizes (which differ by an order of magnitude, see Fig. 6b) the onset of NDTR occurs at the same value of Δ and there is no noticeable difference in the onset or the width of the NDTR region. This size independence of the NDTR here is due to the fact that for the given choice of parameters the system is very

close to the ballistic regime where the thermal current is independent of the system size. The onset of the NDTR phase for different values of the magnetic field occurs at the same value of Δ ; for larger fields the magnitude of resistance seems to be slightly larger.

Many factors have been considered to be relevant for the occurrence of the NDTR regime and these have been analyzed in generic phononic systems recently. In phononic systems, the emergence of the NDTR region has been explained in terms of the mismatch of the phonon bands of the two particles at the interface [8, 9]. This however has its problems, since it was seen that the band overlap does not depend on the system size whereas NDTR seems to disappear for large system sizes [22]. In another work ballistic transport has been thought to be responsible for NDTR and it was shown that an NDTR to PDTR crossover can take place if there is an accompanying ballistic to diffusive crossover [29]. However a subsequent work showed that NDTR can emerge even in absence of such crossover of transport processes [30]. Another work suggested that the increasing interface resistance competes with the increasing temperature gradient and this gives rise to NDTR [28]. The occurrence of the NDTR was thought to be the consequence of the nonlinear response of the lattice which causes the interface resistance to behave nonlinearly for larger thermal gradients. The current increases regularly as the gradient increases but the interface resistance also increases with the gradient. When the decrease in the current due to the interface resistance dominates the increases in current due to the imposed temperature gradient NDTR emerges in such two segment nonlinear systems [28]. From Fig. 5b we find that the energy jump for the two dissimilar lattice increases with the bias. The interface resistance is given as $R_I = \Delta E/J$, where ΔE is the energy jump at the interface and J is the current through the system. However we do not have any means to independently compute both the interface resistance R_I as well as the current J and thus it is not clear how R_I varies as the bias Δ is increased. In Ref. [31], the existence of a critical value for system size N and link interaction constant K_I was considered above which there is no NDTR and a corresponding phase diagram was constructed in the $N \sim K_I$ space. Also it was observed that the interaction at the interface is a crucial factor for NDTR - adding nonlinearity to the link interaction results in the disappearance of NDTR [31]. In the following, we seek to resolve and reconcile these issues using our spin model, and investigate the microscopic mechanism that gives rise to NDTR.

To have a better insight let us first understand the difference between the two cases i.e. $\lambda = 0$ and 1; the former clearly shows NDTR (Fig. 5a) whereas the latter (Fig. 2a) does not, for the same choice of system parameters. Consider only two spins \vec{S}_i and \vec{S}_j ($j = i \pm 1$) which interact via Eq. 3 with $\lambda = 0$. The equations of motion for the two spins are

$$\begin{aligned}\dot{S}_{i,j}^x &= K_I S_{i,j}^y S_{j,i}^z \\ \dot{S}_{i,j}^y &= -K_I S_{i,j}^x S_{j,i}^z \\ \dot{S}_{i,j}^z &= 0.\end{aligned}\tag{10}$$

Thus the equation of motion for both the spins is linear for $\lambda = 0$ whereas it is nonlinear

for $\lambda = 1$. We have simulated our system for intermediate values of λ in the range $0 < \lambda < 1$ and the results are presented in Fig. 7. As expected we find that for smaller λ values, the NDTR regime appears in the $J \sim \Delta$ curve whereas for larger values it vanishes, keeping all other parameters the same. Therefore, it is relatively easy to observe NDTR if the link interaction is linear whereas adding nonlinearity results in the disappearance of NDTR. Also it is clear from Eq. (10) that for $\lambda = 0$ the interface spin stiffness is comparatively larger (since $\dot{S}_{i,j}^z = 0$) and restricts energy flow across the interface; this restriction, we suspect, is responsible for the emergence of NDTR for $\lambda = 0$ and not for $\lambda = 1$, with all system parameters kept the same. Note that in Fig. 7 we have chosen a spatially symmetric lattice and yet exhibits NDTR which clearly shows that asymmetry is not an essential criterion; NDTR can emerge in perfectly symmetric systems. Also, since the system is symmetric, it is straightforward to construct the $J \sim \Delta$ curves shown in Fig. 7 for $0 \leq \Delta \leq 1$.

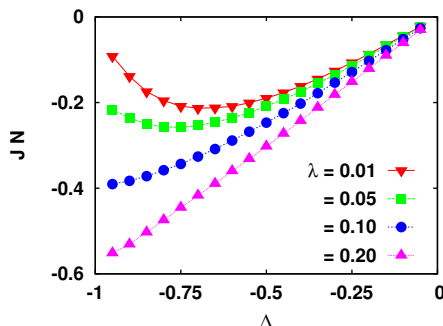


Figure 7. (Color online) The variation of thermal current with Δ in a spatially symmetric lattice for different values of λ . The parameters chosen are $K = 1.0$, $K_I = 1.0$, $h = 1.0$, $T_0 = 1.0$ and segment size $N = 100$. The NDTR regime disappears as λ is increased.

We speculate that any factor which impedes the energy flow through the link should give rise to NDTR. If this is true then even for $\lambda = 1$ we should get NDTR by judiciously tuning system parameters and restricting the current across the link. Since the average current through the i -th bond (between \vec{S}_i and \vec{S}_{i+1}) interacting via \mathcal{H}_I with $\lambda = 1$ (in absence of magnetic fields) can be expressed as $J_i = \langle K_I (\vec{S}_i \times \vec{S}_{i+1}) \cdot \vec{S}_{i+2} \rangle$ [19], the current J_i can be restricted in either of the two ways - (a) by applying high local magnetic fields on spins on either side of the bond (this will make \vec{S}_i almost parallel to \vec{S}_{i+1} and hence $|\vec{S}_i \times \vec{S}_{i+1}| \approx 0$) and (b) by decreasing interaction strength K_I between the two spins \vec{S}_i and \vec{S}_{i+1} . (Recall that the interface resistance is given as $R_I = \Delta E/J$; thus a smaller J across the interface implies larger resistance.) These are applied to the interface spins, \vec{S}_N^L and \vec{S}_1^R , and the results are displayed in Fig. 8a and b respectively. We find that in both cases there is a clear emergence of the NDTR region. Note that the parameters used in Fig. 8a (other than λ) are the same as that of Fig. 7 except for a stronger magnetic field for spins \vec{S}_N^L and \vec{S}_1^R . Likewise for Fig. 8b, all parameters remain the same as in Fig. 7 except for a lower value of the link interaction strength K_I . Thus

in conformity with our proposition, we find that NDTR arises when the energy flow across the link is suitably restricted even if link interaction is highly nonlinear. This mechanism also consistently explains all the parameter dependencies for NDTR. For example in large systems (or equivalently at high temperatures), the transport process approach the diffusive regime and the stiffness of the spins decrease and this eases energy flow across the link which results in the disappearance of NDTR. However, in our system we can make NDTR insensitive to system size (see Fig. 6b) by properly tuning other parameters, such as the local magnetic fields, so that the large spin stiffness at the interface is maintained. Thus this simple physical mechanism satisfactorily explains the

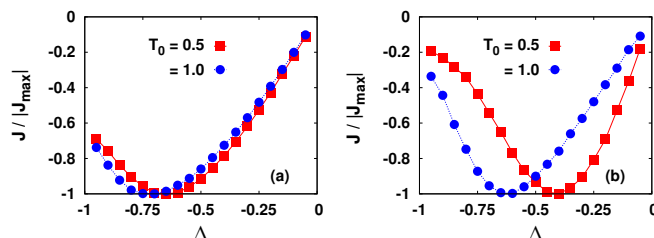


Figure 8. (Color online) The variation of thermal current J with Δ for (a) magnetic field $h = 20.0$ for \vec{S}_N^L and \vec{S}_1^R (for all other spins $h = 1.0$) and other parameters $K = 1.0$, $K_I = 1.0$ and (b) $K_I = 0.01$ with $K = 1.0$, and $h = 1.0$ for all spins. Here $\lambda = 1$ and the current J has been scaled by the maximum (absolute) value of the current $|J_{max}|$ for better comparison. Note that the system is homogeneous (identical spin-spin interaction for all spins in the system) in (a) and segments are spatially symmetric in (b). Here the segment size $N = 100$.

puzzling issues concerning NDTR. We find that our results are consistent with a recent analytical work [38] that also presents a similar idea using a simple particle hop model where such negative responses can emerge naturally due to obstruction, a feature typical of nonequilibrium steady states in driven systems.

5. Conclusion

To summarize, we have performed extensive numerical study of a two segment thermally driven classical Heisenberg spin chain in presence of external magnetic field. The spin couplings and the applied magnetic fields can in general take different values in the left and the right segment. The composite system is thermally driven by attaching heat reservoirs at the two ends. By properly tuning system parameters one can achieve thermal rectification in this system similar to other nonlinear asymmetric systems. Thus the system behaves as a good conductor of thermal energy along one direction but restricts the flow of energy in the opposite direction. The rectification efficiency is found to be controlled by nonlinearity and spatial asymmetry of the lattice.

The rectification of thermal current in such nonlinear asymmetric two segment lattices can be physically interpreted in terms of the interface resistance which is found to be larger in one direction as compared to the other. The rectification efficiency

drops as the system size or the average temperature is increased since a crossover occurs from ballistic to diffusive transport of energy. The decrease in efficiency η is smaller when the system is closer to the ballistic regime and this can be controlled by tuning the external magnetic field accordingly. Thus deep inside the ballistic regime the efficiency is practically independent of the system size or the temperature. At the level of individual spins, we show that the ease of rotation of the interface spins controls the rectification seen in this system.

Besides rectification, negative differential thermal resistance can also emerge in this system where the thermal current decreases as the imposed gradient is increased. This feature emerges in homogeneous, symmetric and asymmetric systems. The underlying mechanism for the appearance of NDTR is the restriction of the current through the link connecting the two segments. This can be tuned by suitably controlling the link interaction \mathcal{H}_I , or other local parameters such as h , K_I . Thus for the emergence of NDTR the crucial features seem to be nonlinearity of the system under investigation and a suitable mechanism to impede the flow of thermal energy in the bulk of the system. This physical mechanism is not restricted to the spin system studied here and should also extend to generic nonlinear systems.

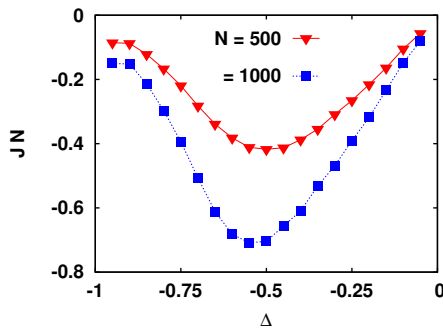


Figure 9. (Color online) The variation of thermal current J with Δ in a homogeneous lattice with $\lambda = 1$ for segment sizes $N = 500$ and 1000 . The magnetic field h for the two interface spins \vec{S}_N^L and \vec{S}_1^R is $h = -20.0$ (along the negative \hat{z} direction) and for all other spins $h = 0.0$; other parameters are $K = 1.0$, $K_I = 1.0$, $T_0 = 0.5$.

We end with a few brief comments on the experimental realization of NDTR. In some of the previous studies [29, 31] it was suggested that NDTR will be difficult to implement in real systems since it is extremely sensitive to interface parameters, temperature and system size. However in view of the discussion presented here we believe that this should not be, in principle, very difficult to fabricate. Transport studies in spin systems are of active experimental interest in recent times [15]. The classical Heisenberg model is realizable in practice and chemical compounds which can be mimic classical Heisenberg interactions are known for quite some time now [39, 40]. In such a chemical system the only requirement seems to be a relatively high external magnetic field at two points close to each other in the bulk which will impede energy flow and give rise to NDTR. We have also verified that this physical mechanism holds also for

large system sizes, as shown in Fig. 9 and is not a finite size effect. This proposed experimental setup is a homogeneous symmetric system and does not require any high precision tuning of the interface properties of the material; only the magnitude of the external magnetic field needs to be properly controlled (see, for example, the parameter values used in Fig. 9). Hopefully, with the recent advancement of low dimensional experimental techniques these theoretical predictions will be verified and lead to the fabrication of devices for efficient thermal management.

Acknowledgments

The author would like to thank P. K. Mohanty for helpful suggestions and careful reading of the manuscript.

References

- [1] N. Li, J. Ren, L. Wang, G. Zhang, P. Hänggi, B. Li, *Rev. Mod. Phys.* **84**, 1045-1066 (2012).
- [2] G. Casati, *Chaos* **15**, 015120 (2005).
- [3] F. Bonetto, J. L. Lebowitz, and L. Rey-Bellet, *Fourier law: A challenge to theorists*, in *Mathematical Physics 2*.
- [4] S. Lepri, R. Livi, and A. Politi, *Phys. Rep.* **377**, 1 (2003).
- [5] A. Dhar, *Advances in Physics*, **57**, 457, (2008).
- [6] M. Terraneo, M. Peyrard, and G. Casati, *Phys. Rev. Lett.* **88**, 094302 (2002).
- [7] B. Li, L. Wang, and G. Casati, *Phys. Rev. Lett.* **93**, 184301 (2004).
- [8] B. Li, L. Wang, and G. Casati, *Appl. Phys. Lett.* **88**, 143501 (2006).
- [9] L. Wang and B. Li, *Phys. Rev. Lett.* **99**, 177208 (2007).
- [10] L. Wang and B. Li, *Phys. Rev. Lett.* **101**, 267203 (2008).
- [11] J. Wu, L. Wang, and B. Li, *Phys. Rev. E* **85**, 061112 (2012).
- [12] C. W. Chang, D. Okawa, A. Majumdar, and A. Zettl, *Science* **314**, 1121 (2006).
- [13] C. W. Chang, D. Okawa, H. Garcia, A. Majumdar, and A. Zettl, *Phys. Rev. Lett.* **99**, 045901 (2007).
- [14] H. Fröhlich, W. Heitler, *Proc. Roy. Soc. (London)* A155, 640 (1936).
- [15] C. Hess, *Eur. Phys. J. Special Topics* **151**, 73 (2007); A. V. Sologubenko, T. Lorenz, H. R. Ott, and A. Freimuth, *J. Low Temp. Phys.* **147**, 387 (2007).
- [16] M. E. Fisher, *Am. J. Phys.* **32**, 343 (1964).
- [17] G. S. Joyce, *Phys. Rev.* **155**, 478 (1967).
- [18] A. V. Savin, G. P. Tsironis, and X. Zotos, *Phys. Rev. B* **72**, 140402(R) (2005).
- [19] D. Bagchi and P. K. Mohanty, *Phys. Rev. B* **86**, 214302 (2012).
- [20] N. A. Roberts and D. G. Walker, *Int. J. Thermal Sci.* **50**, 648 (2011).
- [21] B. Hu, D. He L. Yang and Y. Zhang, *Phys. Rev. E* **74**, 060101(R) (2006).
- [22] B. Hu, L. Yang, and Y. Zhang, *Phys. Rev. Lett.* **97**, 124302 (2006).
- [23] J. Lan, L. Wang, B. Li, *Phys. Rev. Lett.* **95**, 104302 (2005).
- [24] N Yang, N Li, L Wang, and B. Li, *Phys. Rev. B* **76**, 020301(R) (2007).
- [25] J Wang, E. Pereira and G. Casati, *Phys. Rev. E* **86**, 010101(R) (2012).
- [26] J. Lan, B. Li, *Phys. Rev. B* **74**, 214305 (2006).
- [27] J. Lan, B. Li, *Phys. Rev. B* **75**, 214302 (2007).
- [28] D. He, S. Buyukdagli, and B. Hu, *Phys. Rev. B* **80**, 104302 (2009).
- [29] W.-R. Zhong, P. Yang, B.-Q. Ai, Z.-G. Shao, and B. Hu, *Phys. Rev. E* **79**, 050103(R) (2009).
- [30] Z.-G. Shao and L. Yang, *EPL*, **94**, 34004 (2011).

- [31] Z.-G. Shao, L. Yang, H.-K. Chan, and B. Hu, Phys. Rev. E **79**, 061119 (2009).
- [32] D. He, B.-q. Ai, H.-K. Chan, and B. Hu, Phys. Rev. E **81**, 041131 (2010).
- [33] L. Wang and B. Li, Phys. Rev. E **83**, 061128 (2011).
- [34] E Magyari and H Thomas, J. Phys. C: Solid State Phys. **15**, L333 (1982).
- [35] D. Bagchi, Phys. Rev. B **87**, 075133 (2013).
- [36] H. Goldstein, C. P. Poole and J. L. Safko, Classical Mechanics, 3rd Edition, Addison Wesley.
- [37] E. T. Swartz and R. O. Pohl, Rev. Mod. Phys. **61**, 605 (1989).
- [38] R. K. P. Zia, E. L. Praestgaard, and O. G. Mouritsen, Am. J. Phys. **70**, 384 (2002)
- [39] J. L. De Jongh and A.R. Miedema, Adv. Phys. **23**, 1 (1974).
- [40] M. Steiner, J. Villain, and C. Windsor, Adv. Phys. **25**, 87 (1976).